

2006

Development of Air Pump for Fuel Cells

Tatsuya Nakamoto

Matsushita Electric Industrial Co.

Atsushi Sakuda

Matsushita Electric Industrial Co.

Kiyoshi Sawai

Matsushita Electric Industrial Co.

Noboru Iida

Matsushita Electric Industrial Co.

Noriaki Ishii

Osaka Electro-Communication University

Follow this and additional works at: <http://docs.lib.purdue.edu/icec>

Nakamoto, Tatsuya; Sakuda, Atsushi; Sawai, Kiyoshi; Iida, Noboru; and Ishii, Noriaki, "Development of Air Pump for Fuel Cells" (2006). *International Compressor Engineering Conference*. Paper 1784.

<http://docs.lib.purdue.edu/icec/1784>

This document has been made available through Purdue e-Pubs, a service of the Purdue University Libraries. Please contact epubs@purdue.edu for additional information.

Complete proceedings may be acquired in print and on CD-ROM directly from the Ray W. Herrick Laboratories at <https://engineering.purdue.edu/Herrick/Events/orderlit.html>

DEVELOPMENT OF AIR PUMP FOR FUEL CELLS

*Tatsuya Nakamoto¹, Atsushi Sakuda¹, Kiyoshi Sawai¹, Noboru Iida¹, Noriaki Ishii²

¹Refrigeration, Air Conditioning and Heating Research Laboratory,
Matsushita Home Appliance Company, Electric Industrial Co., Ltd.,
2-3-1-1 Nojihigashi, Kusatsu City, Shiga, Japan
Tel.: +81-77-567-9801; Fax: +81-77-561-3201
E-mail: nakamoto.tatsuya@national.jp *Author for Correspondence

²Professor, Faculty of Engineering, Osaka Electro-Communication University,
18-8 Haccho, Neyagawa City, Osaka, Japan
Tel.: +81-728-20-4561; Fax: +81-728-20-4577; E-mail: ishii@isc.osakac.ac.jp

ABSTRACT

In recent years, as the mobile equipment advances, higher output and higher energy density are required of the battery which drives the mobile equipment. As one of the solutions, development of portable fuel cells (DMFC) with methanol used for fuel has been progressed and the fuel cells will be soon put to practical use. The authors have developed a small air pump (0.2W output), which is mounted to DMFC and forcibly feeds air for reactions with methanol. While being oil-less, this air pump achieves an unparalleled small size and high pressure in the world, by adopting a vane rotary type mechanism with two self-lubricating vanes used. In addition, by carrying out dynamic analyses to investigate the vane configuration in the course of developing this pump and by providing several contrivances to the cylinder surfaces on which the vanes slide, low noise and small input were achieved. In this paper, the configuration of developed pump, the developed technique and the results of dynamic analyses, and the pump performance will be reported.

1. INTRODUCTION

In recent years, downsizing and increased functions of mobile information equipment have been amazingly advanced, and for example, notebook PCs not only with personal computer functions but also with AV functions and radio communication functions, have been put on market. As a result, power consumption of mobile information equipment has increased, and battery that drives this equipment must satisfy requirements for higher output and higher energy density. Presently, for this kind of battery, the Li-ion battery is used, but its energy density is almost reaching to its limit. One of the solutions to this problem is mobile fuel cells that use methanol for fuel, and development is positively underway in the world in an effort to put it into practical use in the near future. In the mobile fuel cells, methanol fuel and oxygen (air) are supplied to the power generation section (stack), where methanol fuel is allowed to react chemically with oxygen to generate electric power.

In order to increase the output power of the mobile fuel cells and improve its controllability, it is essential to timely provide necessary and sufficient air amount to the stack. The air pump plays a role to supply air to the stack, and is the most significant device to offer technical advantages on the mobile fuel cells. For the air pump, which is mounted to the mobile fuel cells, characteristics of (1) oil-less operation, (2) small-size, (3) high pressure, (4) low noise and (5) small input power are required. Then, the authors worked to develop small-size and high-performance air pump.

In the first stage of development, efforts were made to choose a compression mechanism. Five kinds of compression mechanism were taken up, and performance, noise, size and reliability are compared. As a result, a rotary vane mechanism was chosen. In this mechanism, the vane transports air while the vane comes in contact with a cylinder wall, then high volumetric efficiency, small size and high discharge pressure may be obtained at a small air flow rate. And also valve-less mechanism may be achievable, which is advantageous from the viewpoint of noise.

In the second stage of development, prototype pump was made, and it was confirmed that the prototype exhibits the initial performance as targeted. In the third stage, to aim at the stabilization of noise and input power, the authors worked for dynamic analysis of the compression mechanism. With this dynamic analysis, the magnitude of the forces acting on the vane and its meaning were clarified. Then, based on analytical results, an original vane sliding form was adopted, which stabilizes noise and input power over a long operation. Through these processes, the authors were able to develop an air pump for mobile fuel cells, which provides features without parallel in the world; that is, small size, considerably high pressure, low noise, and small input. This paper reports the structure of the developed air pump, the process and results of dynamic analysis, unique vane configuration and the pump performance.

2. BASIC STRUCTURE AND FEATURES OF THE AIR PUMP

2.1 Basic structure of the air pump

Figure 1 shows the basic structure of the developed air pump. This air pump adopts a rotary vane system for the compression mechanism, which is driven by a DC motor. The compression mechanism comprises a cylinder, a rotor, vanes, a front plate, and a rear plate. The rotor is arranged in the cylinder in the condition eccentric from the central axis, and to the rotor, two slits are provided, and to these slits, two vanes are fitted in the condition free to slide. The front plate and the rear plate are so arranged that they sandwich these cylinder, rotor, and vanes, thus forming the compression chambers. When the motor-rotor rotates, the rotor rotates via the shaft. And then the vane rotates in contact with the cylinder wall by the centrifugal force and discharge pressure to the rear of the vane. By expanding and contracting of the compression chambers, the pumping action is generated. The air is inhaled through a suction port in the front plate and after the air is pressurized inside the compression chambers, it is discharged through the discharge port in the front plate.

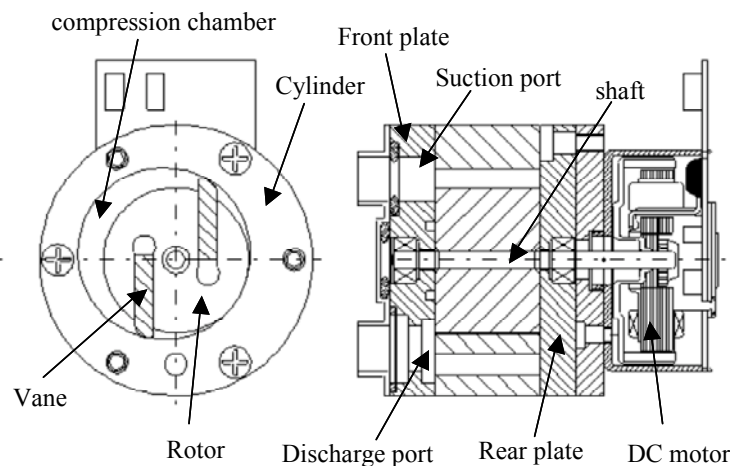


Figure 1: Basic structure of the air pump

2.2 Specifications and features of the air pump

Table 1 shows final specifications of the developed air pump and Figure 2 shows the performance characteristics (P-Q-W characteristics). The first feature of this pump is a small diameter (ϕ 30mm), which is achieved by arranging vanes eccentric from the rotor center as shown in Figure 1. The second feature is a high discharge pressure ($\Delta P = 2 \sim 6$ kPa) and small input power at small flow rate ($Q = 1.5 \sim 4$ L/min). A third feature is a low noise (40dB) achieved by optimizing built-in volume ratio (= suction volume divided by compression end volume) and eliminating a discharge valve. In addition, in order to stably maintain low noise, a unique

Table 1: Final specifications of the air pump

Compression mechanism	Rotary vane	
Displacement volume V	1.5	cc/ rev
Discharge pressure ΔP	2~6	kPa
Air flow rate Q	1.5 ~4	L/min
Power source (DC)	10 ~15	V
Noise at 50cm	40	dB(A)
Size	ϕ 30 \times L 40	mm
Mass	70	g

vane sliding form is adopted. The fourth feature is the vane of this air pump, which is formed with carbon composite material with self-lubricity. With an original surface treatment on the cylinder wall on which the vane slides, a long-time (10,000 hours) oil-less operation has been enabled.

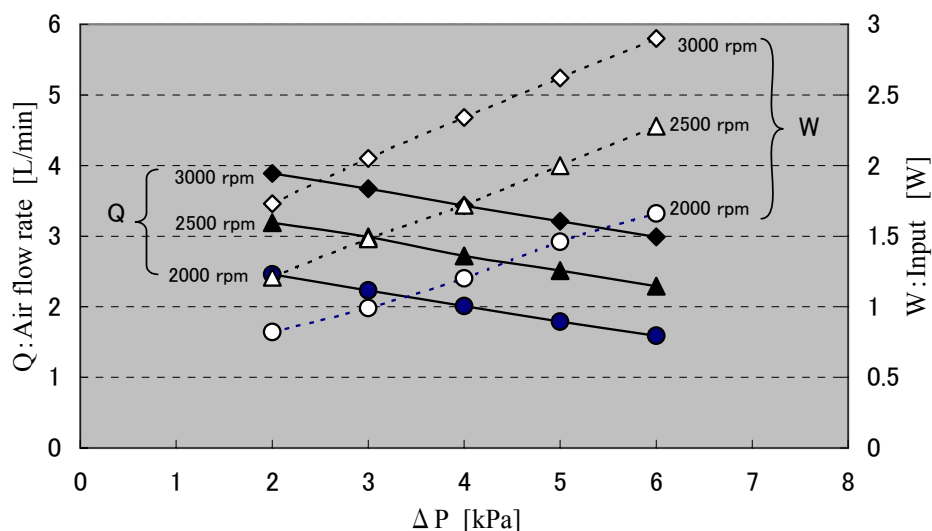


Figure 2: Performance diagram of the air pump (P-Q-W characteristics)

3. DYNAMIC ANALYSIS OF COMPRESSION MECHANISM

3.1 Objectives of the dynamic analysis

The vane moves on the cylinder while the head comes in contact with the cylinder wall. In the case of eccentric arrangement of the vane, there are two types of sliding form as shown in Figure 3. In the event that the angle made by the vane and the cylinder wall is less than 90° , the sliding form is called the “Trailing type”, which in the event that it is larger than 90° , the sliding form is called the “Scooping type.”

It is suggested that the pump characteristics such as noise, compression power, reliability, depend on the vane sliding form. Therefore, in order to make clear the effects of the vane sliding form on the pump characteristics, efforts were made to clarify the forces acting on the vane, that is, dynamic analysis of the vane was carried out.

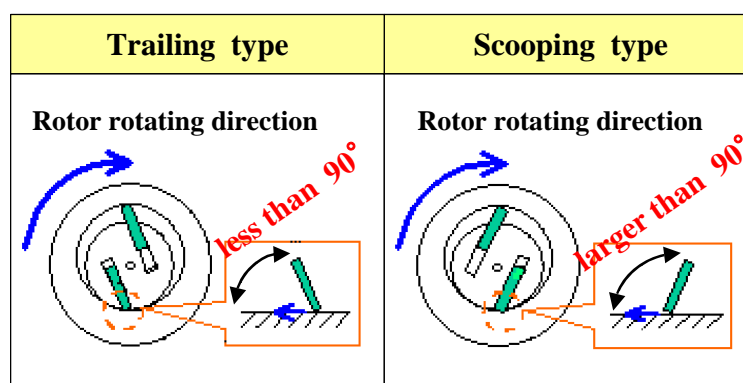


Figure 3: Two types of the vane sliding form

3.2 Process of dynamic analysis

In this section, taking the “Trailing type” vane sliding form for an example, the process of the dynamic analysis is described. The authors worked to develop a technique, with which we can analyze the forces acting on the vane in contact with the cylinder wall or rotor slit. Using the analytical model of the compression mechanism in Figure 4,

the equilibrium of forces moments acting on the vane is formulated, thus resulting in the following equations, respectively.

3.2.1 The region in which the vane comes out from the slit ($\theta : 0-180^\circ$). Equilibrium expression of forces on the vane in the slit direction:

$$F_w \cos(\phi + \phi_0 - \theta) - \mu F_w \sin(\phi + \phi_0 - \theta) + \mu_1 (|R_1| + |R_2|) + (-m_b \ddot{x}_G) \sin \theta + (-m_b \ddot{y}_G) \cos \theta - W1 - W2 + (-2m_b \psi \nu_G) \cos \psi = 0 \quad (1)$$

Equilibrium expression of forces on the vane in the normal direction to the slit.

$$F_w \sin(\phi + \phi_0 - \theta) - \mu F_w \cos(\phi + \phi_0 - \theta) + R_1 - R_2 - (-m_b \ddot{x}_G) \cos \theta + (-m_b \ddot{y}_G) \sin \theta - W3 + (-2m_b \psi \nu_G) \sin \psi = 0 \quad (2)$$

Equilibrium expression of the moment around point G on the vane.

$$\begin{aligned} & -I_b \ddot{\theta} - F_w \{ b \sin(\phi + \phi_0 - \theta) + a \cos(\phi + \phi_0 - \theta) \} - \mu F_w \{ b \sin(\phi + \phi_0 - \theta) - a \sin(\phi + \phi_0 - \theta) + r_b \} \\ & + R_1 (b + \triangle L) + R_2 (L - b) - \mu_1 |R_1| \frac{B}{2} + \mu_1 |R_2| \frac{B}{2} \\ & - W1 \left\{ \frac{B}{2} - \frac{B - r_b \sin(\phi + \phi_0 - \theta) + a}{2} \right\} + W2 \left\{ \frac{B}{2} - \frac{r_b \sin(\phi + \phi_0 - \theta) + \frac{B}{2} - a}{2} \right\} \\ & - W3 \left\{ b + \triangle L + \frac{r_b \cos(\phi + \phi_0 - \theta) - \triangle L}{2} \right\} = 0 \end{aligned} \quad (3)$$

3.2.2 The region in which the vane enters into the slit ($\theta: 180-360^\circ$). Balancing expression of forces on the vane in the slit direction.

$$F_w \cos(\phi + \phi_0 - \theta) - \mu F_w \sin(\phi + \phi_0 - \theta) - \mu_1 (|R_1| + |R_2|) + (-m_b \ddot{x}_G) \sin \theta + (-m_b \ddot{y}_G) \cos \theta - W1 - W2 + (-2m_b \psi \nu_G) \cos \psi = 0 \quad (4)$$

Equilibrium expression of forces on the vane in the normal direction to the slit.

$$F_w \sin(\phi + \phi_0 - \theta) - \mu F_w \cos(\phi + \phi_0 - \theta) + R_1 - R_2 - (-m_b \ddot{x}_G) \cos \theta + (-m_b \ddot{y}_G) \sin \theta - W3 + (-2m_b \psi \nu_G) \sin \psi = 0 \quad (5)$$

Equilibrium expression of the moment around point G on the vane.

$$\begin{aligned} & -I_b \ddot{\theta} - F_w \{ b \sin(\phi + \phi_0 - \theta) + a \cos(\phi + \phi_0 - \theta) \} - \mu F_w \{ b \sin(\phi + \phi_0 - \theta) - a \sin(\phi + \phi_0 - \theta) + r_b \} \\ & + R_1 (b + \triangle L) + R_2 (L - b) + \mu_1 |R_1| \frac{B}{2} - \mu_1 |R_2| \frac{B}{2} \\ & - W1 \left\{ \frac{B}{2} - \frac{B - r_b \sin(\phi + \phi_0 - \theta) + a}{2} \right\} + W2 \left\{ \frac{B}{2} - \frac{r_b \sin(\phi + \phi_0 - \theta) + \frac{B}{2} - a}{2} \right\} \\ & - W3 \left\{ b + \triangle L + \frac{r_b \cos(\phi + \phi_0 - \theta) - \triangle L}{2} \right\} = 0 \end{aligned} \quad (6)$$

W1, W2, and W3 are the force that acts on vane, and the cause is a difference of pressure in the compression chamber. These force is estimated by the following equations.

$$W1 = \triangle P1 \left\{ \frac{B}{2} - r_b \sin(\phi + \phi_0 - \theta) + a \right\} H \quad (7)$$

$$W2 = \triangle P2 \left\{ r_b \sin(\phi + \phi_0 - \theta) + \frac{B}{2} - a \right\} H \quad (8)$$

$$W3 = \triangle P3 \left\{ r_b \cos(\phi + \phi_0 - \theta) - \triangle L \right\} H \quad (9)$$

By simultaneously solving equations from (1) to (3) or from(4) to (6) by using expressions from (7) to (9), it is possible to find out the constraint forces R1, R2, and Fw with respect to each rotating angle ($\phi + \phi_0$) of the rotor. These calculations can be easily performed on the personal computer. In addition, from R1 and R2, which are reaction forces acting on vane side by the slit, the compression power can be calculated.

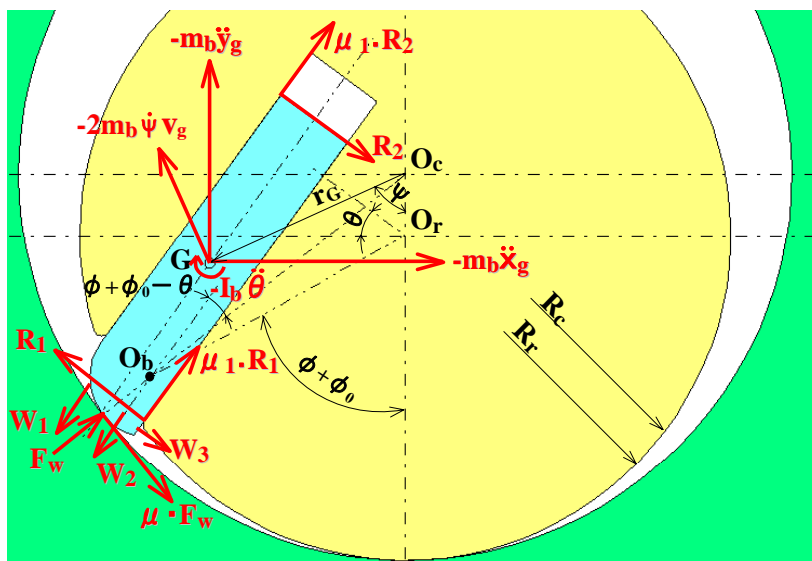


Figure 4: Analytical model of the compression mechanism (Trailing type region in which the vane enters into the slit)

Table 2: Main specifications and Conditions in dynamic analysis

Comp. Spec.	Number of vane	2	—
	Suction volume	1.5	cc/rev
	Vane mass	0.4	g/piece
Anal. Cond.	Discharge pressure ΔP	4	kPa
	Rotational speed N	2,300	r/min
	Frictional coeffi. μ	0.2~0.45	—
	Frictional coeffi. μ_1	0.2~0.45	—

3.3 Results of dynamic analysis

Table 2 shows major specifications of the pump and analytical conditions in dynamic analysis. The forces acting on the vane were analyzed on both “Trailing type” vane and “Scooping type” vane. Figure 5 shows the analytical results of the reaction force Fw in the case of “Scooping type” vane, and Figure 6 shows that in the case of “Trailing type” vane.

In general, in the case of “Scooping type” vane, the friction acting on the vane head works to prevent the vane from coming out from the slit. This analytical results indicate that when the frictional coefficient μ_1 between the vane side and the slit increases, the reactive force Fw by the cylinder wall becomes extremely small at rotating angles 120° to 180° . This suggests that the friction acting on the vane side degrades a smooth slide of the vane in the slit and the vane may not come in contact with the cylinder wall. That is, in the case of the “Scooping type” vane, jumping phenomena occur in actual operation, and as a result, the noise would increase or the air would leak around the vane head, and then the performance would decrease.

On the other hand, in the case of “Trailing type” vane, in general, the friction acting on the vane head works to help the vane come out from the slit. This analytical results evidence that because in the case of “Trailing type” vane, there is no region in which the reaction force Fw approaches to zero even when the frictional coefficient μ or μ_1 varies, the jumping phenomena never occur and the stable low noise is maintained.

However, it has been found that when the frictional coefficient μ or μ_1 increases, the reaction force F_w increases in the region where the vane enters into the slit (rotating angle: 180-300°). When the reaction force F_w increases, there is a fear of increasing the compression power, to which care must be taken.

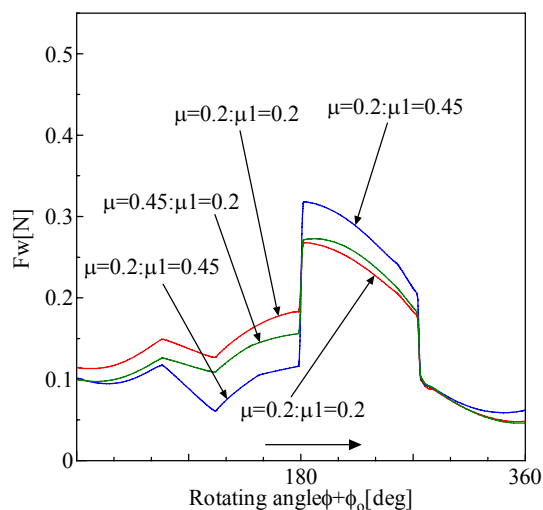


Figure 5: Reactive force acting on the vane by the cylinder wall (Scooping type)

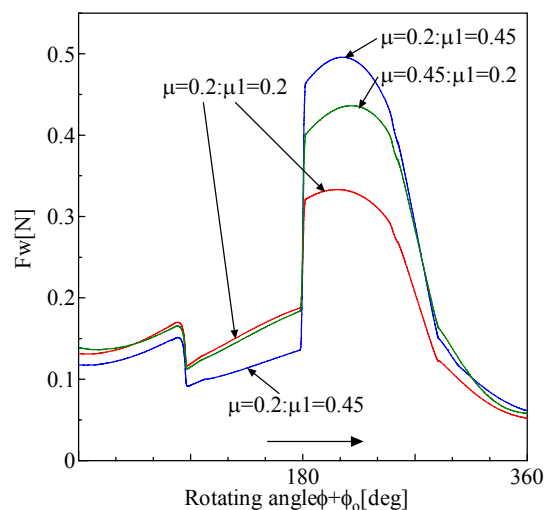


Figure 6: Reactive force acting on the vane by the cylinder wall (Trailing type)

4. EXPERIMENTAL INVESTIGATION OF PERFORMANCE

In order to verify the analytical results, two prototypes of the air pump were made, which has the different kind of vane sliding form. Long-time (400 or 800 hours) operations were carried out, and changes of pump performance were investigated. Figure 7 shows the experimental results of the noise change characteristics, and Figure 8 shows the experimental results of the input power change characteristics.

4.1 Noise change characteristics

The pump with “Scooping type” vane gradually increased noise at 100 hours after the operation was started, and increased noise by about 20dB (A) after 400 hours. On the other hand, in the case of “Trailing type” vane, the pump stably maintained low noise over 800 hours. These results indicate that the increase of noise in the “Scooping type” was caused by the jumping phenomena of the vane.

4.2 Input change characteristics

In the case of the pump with the “Scooping type” vane, small input was stably maintained, whereas in the case of the “Trailing type,” the increasing phenomenon of the input appeared after 100 hours. It is considered that this phenomenon is due to the increase of frictional coefficient μ_1 as in the case of the increase of noise on the “Scooping type.” The increase ratio of the input in the case of “Trailing type” is as large as 50%. But, since the absolute value of the input after the long operation is as small as 1.5W, it is considered that this wouldn't cause any problem in actual uses. These experimental results of noise characteristics and input characteristics were compared with the dynamic analysis results discussed before, and conclusively, the “Trailing type” was chosen as the appropriate vane sliding form.

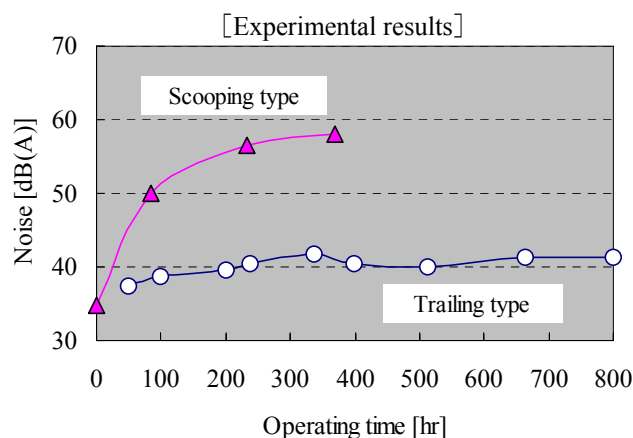


Figure 7: Noise change characteristics of the air pump

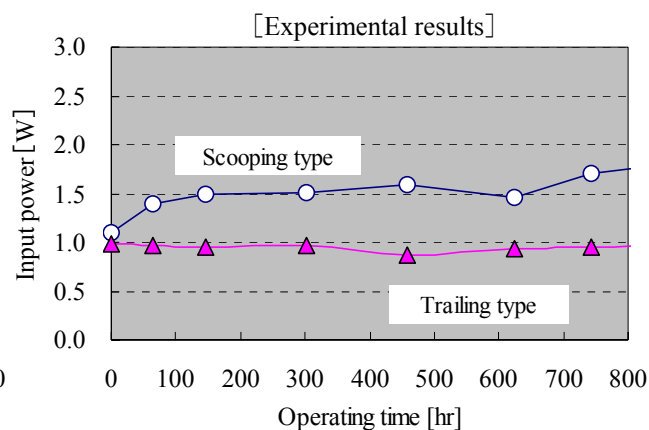


Figure 8: Input power change characteristics of the air pump

With these development processes, the authors were able to develop an air pump for mobile fuel cells with excellent features such as small size, low noise and small input power, which have never been realized before.

6. CONCLUSIONS

We made efforts to develop a small size rotary vane type air pump with high performance for mobile fuel cells, and the following conclusions were obtained.

- An analytical method was introduced to calculate the forces acting on the vane. It has been confirmed that the analytical results are effective for investigation of noises around the vane.
- In the rotary vane type air pump, which operates under the oil-less atmosphere, by adopting “Trailing type” vane, the vane jumping phenomena can be prevented and long time noise stabilization is achieved.

By the way, for this air pump, various kinds of reliability tests are presently underway. We hope that this air pump will put into practical use in the near future, and offer the advantages on the mobile fuel cells.

NOMENCLATURE

V	Displacement volume (cc/rev)
ΔP	Discharge pressure (kPa)
Q	Air flow rate (L/min)
W	Input (W)
F_w	Reactive force by the cylinder wall acting on vane head (N)
ϕ	Rotating angle of the vane (degree)
ϕ_0	Rotating angle of the vane [$\theta = 0$](degree)
θ	Rotating angle of the rotor (degree)
μ	Frictional coefficient between vane head and cylinder wall (-)
μ_1	Frictional coefficient between vane side and slit (-)
R_1	Reactive force acting on vane side by the slit [at the head of the vane] (N)
R_2	Reactive force acting on vane side by the slit [at the rear of the vane] (N)
m_b	Mass of the vane (g)
\ddot{x}_G	Acceleration of vane [x axis direction](m/s ²)
\ddot{y}_G	Acceleration of vane [y axis direction](m/s ²)

W1	Force acting on the vane by rear pressure [part of discharge pressure at the vane head] (N)
W2	Force acting on the vane by rear pressure [part of suction pressure at the vane head] (N)
W3	Force acting on the vane head by discharge pressure (N)
$\dot{\psi}$	Angular velocity of the rotor [around O_c] (rad/s)
v_G	Velocity of the vane (m/s)
I_b	Moment of inertia of vane [around G](Nm)
$\ddot{\theta}$	Angular acceleration of rotor (m/s ²)
a	Distance from circular arc of vane center to center of gravity of vane [Perpendicular direction] (mm)
b	Distance from circular arc of vane center to center of gravity of vane [Rotor radial] (mm)
r_b	Radius circular arc in vane head (mm)
ΔL	Vane length between contact point of Behn side and rotor slit [head side of vane] (mm)
L	Vane length (mm)
B	Vane thickness, Slit width (mm)
H	Cylinder height, Rotor height, Vane height (mm)
Δp_1	Pressure difference of rear pressure and head pressure [direction of rotation side] (kPa)
Δp_2	Pressure difference of rear pressure and head pressure [direction of anti-rotation side] (kPa)
Δp_3	Pressure difference between discharge and suction (kPa)
R_c	Center of inside diameter of the cylinder (mm)
R_r	Center of inside diameter of the rotor (mm)
O_c	Center of the cylinder (-)
O_r	Center of the rotor (-)
r_G	Length from O_c to G (mm)
G	Center of gravity of the vane(-)
O_b	Center of circular arc of vane head (-)
ψ	Rotating angle of the vane around O_c (degree)

REFERENCES

- Sawai, K., Sakuda, A., Nakamoto, T., Iida, N., Tsujimoto, T., Nagata, T., Ishii, N., 2005, Development of Small Size Air Pump for Mobile Fuel Cells, *International Conference on Compressors and their Systems*, Cass Business School, City University, London, UK, C639-27.
- Honda, I., Kanazawa, K., Ooba, H., Kondo, T., Nakashima, Y., 1991, A study on a Sliding Vane-Type Compressor, *TRANS. JSME*, vol. 57, No.534, p.168-172.
- Fukuta, M., Tanaka, M., Shimizu, T., Yanagisawa, T., 1991, Analysis of Film on Vane Slides of Vane Compressors, *TRANS. JSME*, vol. 57, No.538, 81p.

ACKNOWLEDGEMENT

The authors would like to express their sincere thanks to Y.Kanemitsu, T.Tsujimoto, H.Fukuhara, H.Murakami, T.Nagata, Y.Takeuchi for their supports in developing the present small size air pump for mobile fuel cells with small size and high performance.